ELSEVIER

International Journal of Pharmaceutics 104 (1994) 29–40

international journal of pharmaceutics

Kinetics and mechanism of hydrolysis of tyrphostins

Chong Min Won

Analytical and Physical Chemistry Department, Rhône-Poulenc Rorer Central Research, 500 Arcola Road, Collegeville, PA 19426, USA

(Received 16 October 1992; Modified version received 12 April 1993; Accepted 31 August 1993)

Abstract

The rates of hydrolysis of RG 14620, a tyrphostin, have been determined at pH values between 1 and 10. The log k-pH profile shows the rate of the hydrolysis is proportional to the concentration of hydroxide ion above pH 5. In the acidic pH region, the profile shows a curve with a maximum between pH 2 and 3. The presence of a maximum has been interpreted in terms of a change from the rate-determining formation of a tetrahedral addition intermediate on the basic side of the maximum to the rate-determining cleavage of the intermediate on the acidic side. This interpretation is supported by the observations that the reaction is catalyzed by chloroacetate buffer at pH 3.2 and that the catalytic constants for the buffer decrease with an increasing buffer concentration at pH values in the range of 2.26–2.79. The non-linearity is due to the uncatalyzed cleavage of the intermediate which becomes partially rate-determining at higher buffer concentrations. The effect of variation in the polar nature of phenyl substituents at the β-carbon atom of the tyrphostin is in accord with the hydrolysis mechanism.

Key words: Tyrphostin; Kinetics; Mechanism; Hydrolysis

1. Introduction

A series of synthetic compounds called tyrphostins are tyrosine kinase inhibitors which inhibit the kinase activity of the epidermal growth factor receptor in vitro (Lyall et al., 1989). One of the tyrphostins, RG 14620 (*Z*)-2-(3-pyridyl)-3-(3,5-dichlorophenyl)-2-propenitrile (I)) is being developed for the treatment of psoriasis.

Carbon-carbon double bonds activated by electron-withdrawing substituents are susceptible to nucleophilic attack by a variety of nucleophilic reagents on the positively polarized β-carbon atom of the double bond (Patai and Rappoport, 1962). A tyrphostin contains a carbon–carbon double bond activated at the β-carbon atom by an electron-withdrawing cyano substituent (Scheme 1). The double bond undergoes hydration and subsequent bond cleavage that leads to an aldehyde and a methylene compound. Interest in the chemical reactivity of tyrphostins in aqueous solution has led to an examination of the rate and possible mechanism of the hydrolysis and the effect of structural variation upon the hydrolysis rate.

2. Materials and methods

2.1. Materials

RG 14620 (I) was synthesized and supplied by the Process Research and Development Department of Rhône-Poulenc Rorer Central Research

SSDI 0378-5173(93)E0270-Z

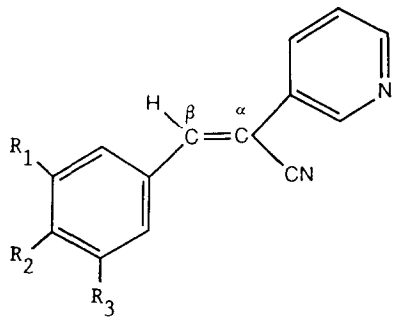

	R_1	R_2	R_3
I	Cl	H	Cl
II	H	H	H
III	H	NO_2	H
IV	H	OCH_3	H

Scheme 1.

and used as received. The other tyrphostins (II–IV; Scheme 1) were prepared by reacting 3-pyridyl acetonitrile with appropriate aldehydes (benzaldehyde, *p*-anisaldehyde, or *p*-nitrobenzaldehyde) as described for II below. The chemicals were purchased from Aldrich Chemical (Milwaukee, WI).

To a solution of benzaldehyde (10 mmol, 1.06 g) in 5 ml of methanol was added 3-pyridyl acetonitrile (10 mmol, 1.18 g). Anhydrous sodium carbonate (100 mg) was added to the solution. The mixture was stirred at room temperature for 20 h and then filtered. The filtrate was evaporated under reduced pressure. The residue obtained was recrystallized twice from 50% methanol in water. A needle-like white crystalline material was obtained. The material was dried at 60°C under vacuum for 2 h.

The ^{1}H-NMR and mass spectra of the compounds were consistent with their structures. HPLC analysis at a detection wavelength of 254 nm revealed II and IV to be free from impurities. Compound III contained approx. 2% of an impurity as determined by HPLC. Elemental analysis results of the compounds are listed in Table 1.

2.2. HPLC analysis

A reversed-phase HPLC procedure was used for the quantitative determination of I. The chromatography system consisted of a pump (Perkin Elmer 410), an automatic injector (Perkin Elmer ISS 100), a diode array detector (Perkin Elmer 480), and a networking computer system (Waters 860). The HPLC method employed a 250 × 4.6 mm i.d. 5 μm particle size, octyl-bonded silica stationary phase column which is sterically protected (Zorbax Rx-C8) and a mobile phase consisting of acetonitrile : water : acetic acid (600 : 400 : 1 v/v). The flow rate was 1.5 ml/min and the detector wavelength for UV absorbance detection was 306 nm.

Table 1
Analytical data of the synthesized tyrphostins

Compound	Melting point (°C)	Formula	Analysis (%)		
				Calculated	Found
II	102–103	$C_{14}H_{10}N_2$	C	81.53	81.39
			H	4.89	4.75
			N	13.58	13.58
III	149–151	$C_{14}H_9N_3O_2$	C	66.93	66.42
			H	3.61	3.53
			N	16.73	16.07
IV	114–115	$C_{15}H_{12}N_2O$, 0.5 H_2O	C	73.45	74.55
			H	5.34	4.96
			N	11.42	11.42

For the analysis of the other tyrphostins, II–IV, a 250 × 4.6 mm i.d. 5 μm particle size, cyano-bonded silica stationary phase column (Zorbax CN) and a mobile phase consisting of acetonitrile : water : acetic acid (450 : 550 : 1 v/v) were used. The detection wavelengths for II, III, and IV were 309, 327, and 337 nm, respectively.

2.3. Kinetic method

Stock solutions of I–IV (100 μg/ml) in acetonitrile as well as buffers (0.2 M) in water were prepared. An aliquot (0.5 ml) of the tyrphostin stock solution, an appropriate amount of hydrochloric acid (pH 1.1–2.0), chloroacetate (pH 2.2–3.2), acetate (pH 3.9–5.1), phosphate (pH 6.1–7.3), borate (pH 8.3–9.7), or carbonate (pH 9.4–9.9) buffer stock solution and an appropriate amount of 1 M NaCl to maintain an ionic strength of 0.1 were transferred into a 100-ml volumetric flask and filled to volume with water. A low buffer concentration of 0.02 M was used to minimize possible general acid-base catalysis by the buffer species. The pH values of the buffer solutions were measured at the reaction temperature with a pH meter standardized at the same temperature. The pH values of HCl solutions at the reaction temperature were calculated from activity coefficients extrapolated from literature data (Harned and Owen, 1958). The reaction flask was kept in a constant-temperature water bath at 80°C (±0.5°C). Samples were taken at appropriate time intervals and an aliquot (150 μl) of the sample was analyzed by HPLC. The compounds are sensitive to photoisomerization and the solutions were protected from light throughout the experiment.

2.4. Determination of pK_a

The low solubility of I in water necessitated the use of the solubility method (Albert and Serjeant, 1971) for the determination of the ionization constant. The equilibrium solubility of I was measured in chloroacetate (pH 3.0–3.5), acetate (pH 4.1–5.2) or phosphate (pH 6.0–6.7) buffer solution at room temperature. All buffer solutions were prepared to have an ionic strength of 0.1. The solubilities measured at various pH values were: pH, solubility (μg/ml); 6.71, 0.34; 6.07, 0.35; 5.21, 0.32; 4.73, 0.38; 4.43, 0.44; 4.10, 0.52; 3.48, 0.98; and 3.00, 2.20. The solubility of I is independent of pH above 4 and increases with decreasing pH below 4 indicating the ionization of I. The estimated pK_a from the solubility data is 3.80.

3. Results and discussion

Using the HPLC conditions described previously, the tyrphostins were separated from the hydrolysis products and isomers. The two degradation products, the aldehyde and methylene compound (Scheme 2), are also the precursors in the synthesis of I. At high concentrations of I, the reaction is reversible. At low concentrations as in this study, the probability of the molecules of the two degradates colliding to produce I is minimal and the reaction appears to be essentially irreversible. The hydrolytic degradation reaction obeyed first-order kinetics through two or more half-lives.

In chloroacetate buffer solutions, the first-order plots for the degradation of II and IV were found to be biphasic showing a rapid initial decrease in the peak area of the substrates followed by a slower second phase. The HPLC chromatogram showed that the rapid decrease in the peak area was accompanied by a rapid increase in the peak area of the corresponding *cis*-isomers which was followed by a slower production of the hydrolysis products.

The compounds II and IV undergo *cis-trans* isomerization in the presence of nucleophiles concurrent with hydrolysis. The positively polarized β-carbon atom of the double bond is attacked by a nucleophile resulting in the formation of a carbanion. The *cis-trans* isomerization occurs readily because it involves only an inversion of the configuration in the carbanion. Its subsequent elimination of the nucleophile from the carbanion permits the isomerization of the compounds. The isomerization was found to be significantly catalyzed by general bases such as chloroacetate ion. General bases can attack the double bond

introduced into the rate constants by neglecting buffer catalysis under the conditions of these experiments (0.02 M buffer concentration) is about 5%.

In neutral and alkaline pH regions (pH > 5), the log k-pH plot is linear with a slope of unity indicating specific hydroxide-ion catalysis (Fig. 1). Under more acidic conditions (pH 3–5), in which the substrate is partly converted to its conjugate acid, the hydrolysis rate increases with increasing acidity. In this pH region, a water attack on the protonated substrate must become the predominant reaction path. Under conditions in which the substrate is completely converted to its conju-

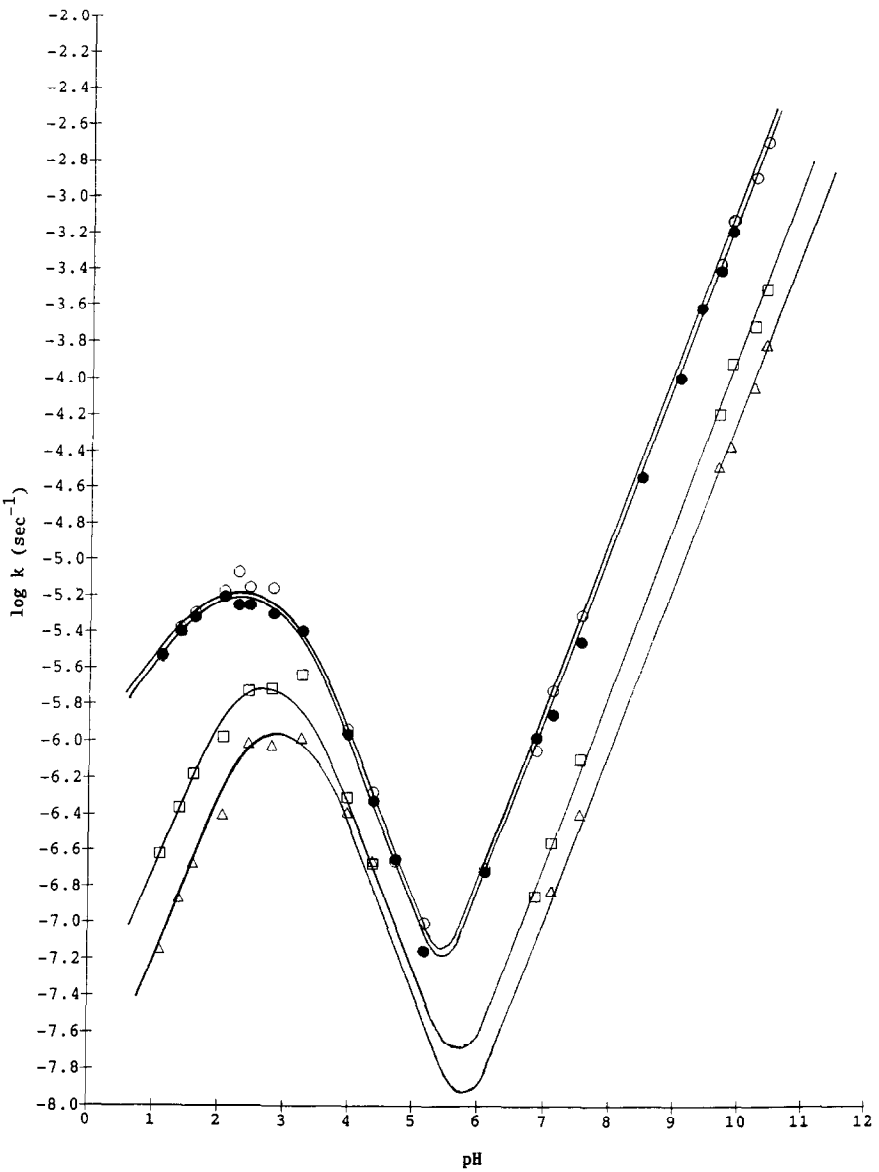

Fig. 1. Logarithm of the first-order rate constants for the hydrolysis of tyrphostins as a function of pH at 80.0°C. Ionic strength maintained at 0.1 by the addition of NaCl. I (●), II (□), III (○) and IV (△). The solid lines were calculated by substituting the constants in Table 2 into Eq. 2 or 6.

gate acid, the hydrolysis rate becomes independent of pH reflecting the rate of the water attack on the fully protonated substrate. At pH values below 2, the hydrolysis rate decreases with increasing acidity and eventually becomes first-order with respect to the hydroxide-ion activity.

The decrease in the rates of many hydrolytic reactions such as amide hydrolysis in strongly acidic solutions (pH below 1) has frequently been explained on the basis of a decrease in the activity of water, which acts as both nucleophilic and proton transfer agent (Bruice and Benkovic, 1966). With tyrphostins, the rate decrease occurs in acidities where the activity of water is still nearly unity and, therefore, an interpretation in terms of decreasing water activity is difficult. In order to account for the rate decrease with increasing acidity for the acidic side of the maximum, it was necessary to postulate the existence of an unstable intermediate in the reaction path-

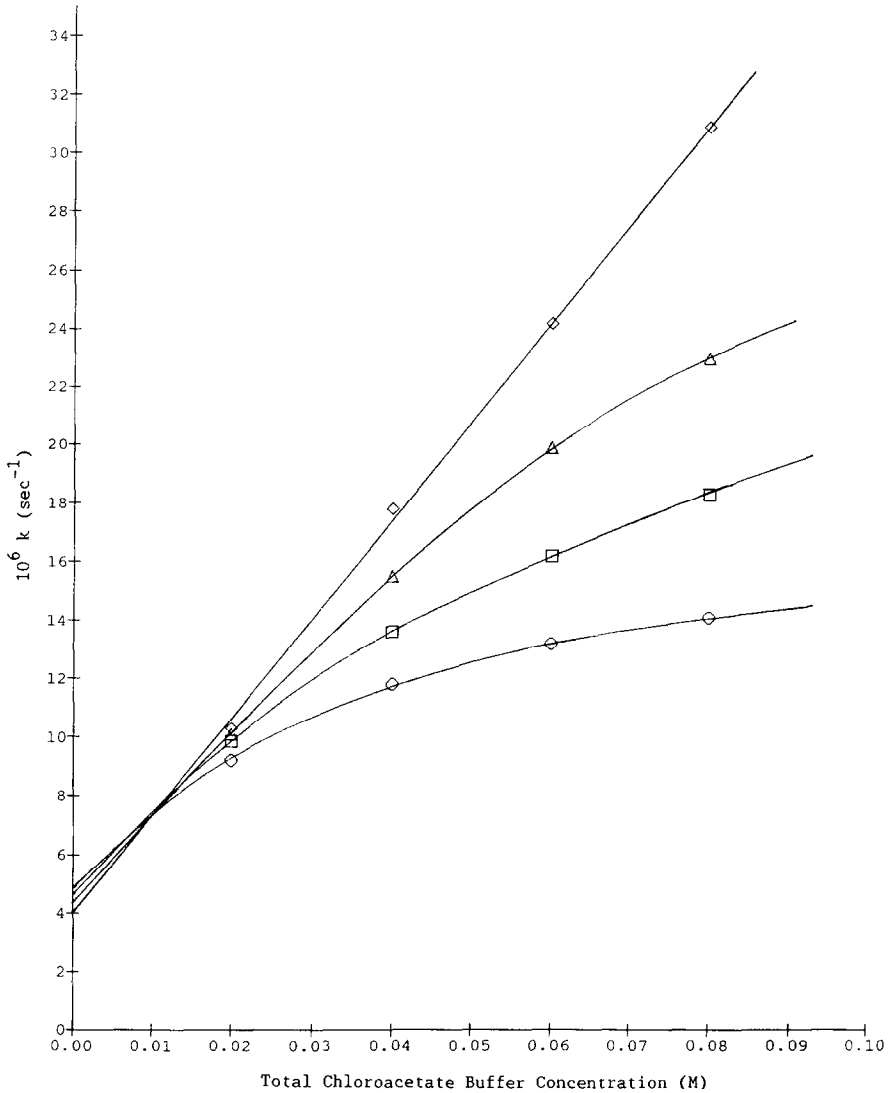

Fig. 2. First-order rate constants at 80.0°C for the hydrolysis of I in chloroacetate buffer as a function of total buffer concentration. pH 2.26 (○), 2.43 (□), 2.79 (△) and 3.24 (◇).

way with the formation and decomposition of the intermediate having different sensitivities to hydronium ion. A possible mechanism for the hydrolysis at pH below 5 is:

$$S + H^+ \rightleftharpoons SH^+$$

$$SH^+ + H_2O + B \underset{k_2}{\overset{k_1}{\rightleftharpoons}} SHOH + HB$$

$$SHOH \xrightarrow{k_3} \text{products}$$

where B and HB are general bases and their conjugate acids, respectively. In weakly acidic solutions, the k_1 step may be rate-determining. In solutions of sufficient acidity, an equilibrium will prevail in the first step resulting in the k_3 step becoming rate-determining. On chemical grounds, the tetrahedral addition compound ($SHOH_2^+$) would most likely be the unstable intermediate (Scheme 2).

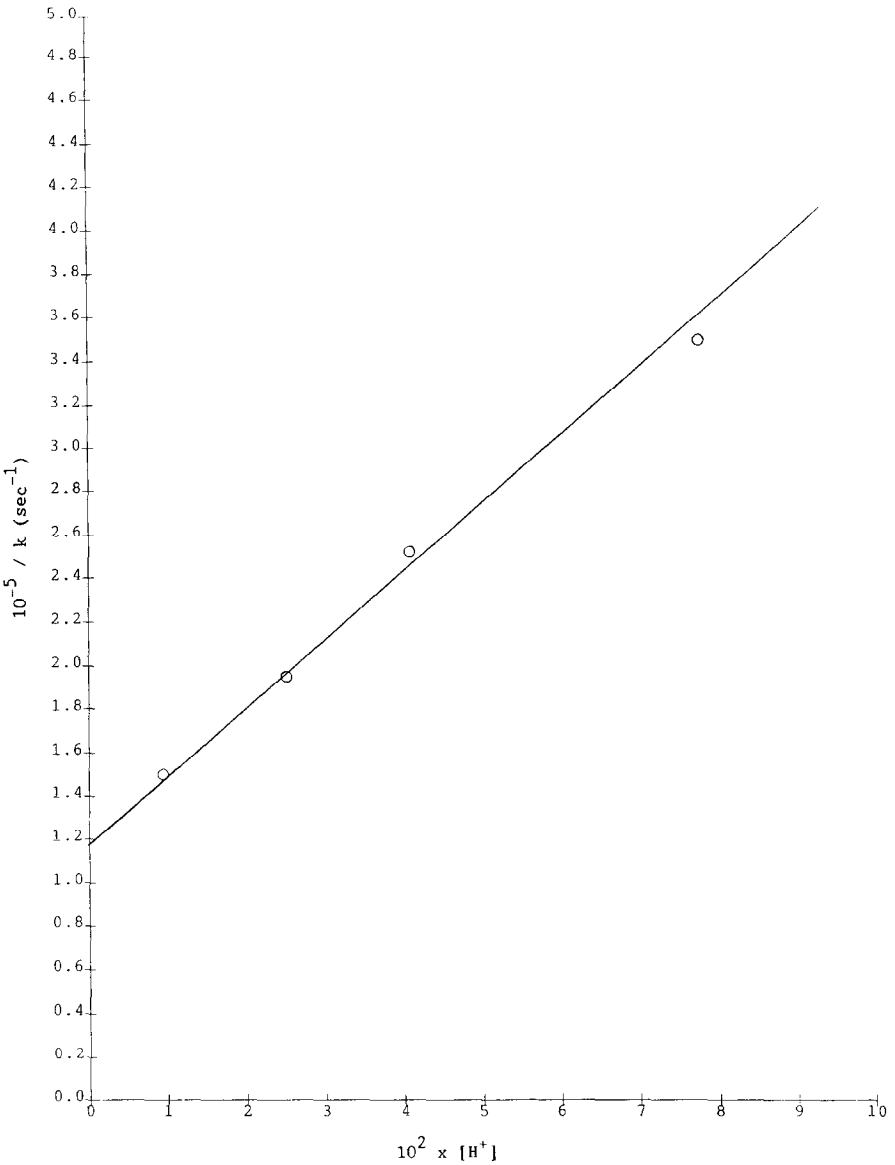

Fig. 3. Linear relationship between $[H^+]$ and $1/k$ for the hydrolysis of I according to Eq. 4.

Application of the steady-state approximation to the deprotonated tetrahedral intermediate (SHOH) yields:

$$k = \frac{f_{SH} k_3 k_1}{k_3 + k_2} = \frac{f_{SH} k_3 \sum k_1'[B]}{k_3 + \sum k_2'[HB]} \quad (1)$$

where k is the observed first-order rate constant, k_1' and k_2' are the catalytic rate constants of the different general bases and acids, respectively, and f is the fraction of the protonated substrate given by $f_{SH} = [H^+]/([H^+] + K_a)$.

In the absence of buffer catalysis, Eq. 1 reduces to:

$$k = \frac{f_{SH} k_1 k_3}{k_3 + k_H[H^+]} \quad (2)$$

where k_H is the catalytic rate constant of H^+.

Between pH 1 and 2, $[H^+] \gg K_a$ and Eq. 2 reduces to:

$$k = \frac{k_1 k_3}{k_3 + k_H[H^+]} \quad (3)$$

When Eq. 3 is converted into its reciprocal form, Eq. 4 is obtained:

$$\frac{1}{k} = \frac{k_H[H^+]}{k_1 k_3} + \frac{1}{k_1} \quad (4)$$

Consequently, the values of k_1 and k_3/k_H were estimated to be 8.8×10^{-6} s^{-1} and 3.0×10^{-2} M, respectively, from the intercept and slope of the linear relationship between $[H^+]$ and $1/k$ for I (Fig. 3).

Between pH 4 and 5, $k_3/k_H \gg [H^+]$ and Eq. 2 reduces to:

$$k = \frac{k_1[H^+]}{[H^+] + K_a} \quad (5)$$

Substituting the value of k_1 into Eq. 5, K_a was estimated to be 7.0×10^{-4}. Considering the temperature effect on the pK_a of pyridines (Albert and Serjeant, 1971), the agreement between kinetic and solubility pK_a values is quite satisfactory.

Table 2
Rate constants for hydrolysis of tyrphostins at 80°C and ionic strength of 0.1

	k_1 ($\times 10^6$) (s^{-1})	k_3/k_H ($\times 10^3$) (M)	k_4' ($\times 10^2$) (s^{-1} M^{-1})
I	8.8	30	50
II	4.6	3.8	7.7
III	9.3	35	55
IV	3.6	1.4	3.8

At pH values above 6, the hydrolysis is the result of direct hydroxide ion attack on the free base:

$$S + OH^- + H_2O \xrightarrow{k_4} \text{products}$$

$$k = k_4 = k_4'[OH^-] = \frac{k_4' k_w}{[H^+]} \quad (6)$$

where k_4' is the catalytic rate constant for the hydroxide-ion attack on the unprotonated substrate.

The logarithmic transformation of Eq. 6 yields:

$$\log k = \log k_4' - pK_w + pH \quad (7)$$

so that the slope of the log k-pH profile (Fig. 1) is equal to unity, and k_4' was estimated to be 5.0×10^{-1} s^{-1} M^{-1} from the plot. The best values of the rate constants for II–IV were obtained by fitting the observed rate constants to the rate equations and the values are presented in Table 2. The solid lines in Fig. 1 are theoretical curves calculated from Eq. 1 or 6 using the constants. The theoretical curves show a good agreement with the observed data.

On the basic side of the maximum in the log k-pH profile, the formation of the tetrahedral addition intermediate is rate-determining, while on the acidic side of the maximum the decomposition of the intermediate is rate-determining. Decomposition of the intermediate requires that the intermediate lose its proton to form the dipolar structure (SHOH) to obtain sufficient driving force for decomposition. Removing the proton from the oxygen atom of the intermediate becomes progressively more difficult in acid solutions. When the rate of the decomposition becomes, because of the difficulty, slower than the pH-independent rate of water attack on the pro-

tonated substrate, a change in rate-determining step occurs and the observed rate decreases with increasing acidity. Similar interpretations of the log k-pH profiles have been presented for the hydrolysis of aliphatic Schiff bases (Cordes and Jencks, 1963; Koehler et al., 1964), 2-methyloxazoline (Martin and Parcell, 1961a; Martin et al., 1964) and 2-methylthiazoline (Martin and Parcell, 1961b). The considerable body of evidence which supports the postulated change in the rate-determining step with pH has been discussed by Jencks (1964) and Martin (1964).

The catalytic effect of hydroxide ion in neutral and alkaline pH regions is due to the greater nucleophilicity of hydroxide ion relative to water towards the positively-polarized β-carbon atom.

The hydrolysis of tyrphostins is catalyzed by chloroacetate buffer. Fig. 2 shows a plot of the observed first-order rate constant of the hydrolysis of I vs total chloroacetate buffer concentration at four different pH values in the plateau region. The increase in catalysis with increasing pH reflects the fact that the active catalytic species is chloroacetate ion. A significant aspect of the chloroacetate buffer catalysis is the non-linear dependence of the rate of hydrolysis upon the total buffer concentration at a fixed pH near the maximum. There is a sharp increase in the rate constant with increasing buffer concentration at low buffer concentrations, but as the buffer concentration is increased, there is a break in the curves and the rate constant increase is reduced indicating less dependence on the buffer concentration. The rate constant eventually levels off and tends to become independent of the buffer concentration at high buffer concentrations. The tendency of the reaction rate to reach a limiting value at a high buffer concentration is seen at all pH values except at pH 3.24, although it is most pronounced at the lowest pH 2.26.

Since no self-association of the buffer system is expected at these concentrations in aqueous solutions, the non-linear variation of rate with an increasing buffer concentration cannot be accounted for by a one-step mechanism and is evidence for a change in the rate-determining step of a reaction with increasing buffer concentration (Jencks, 1969). The formation of the intermediate is rate-determining at low buffer concentrations. The buffer has supplied sufficient catalysis at high buffer concentrations causing the rate of the formation step to become so fast that the breakdown step becomes rate-determining. Additional buffer is ineffective in catalyzing the hydrolytic reaction when the rate of carbon-carbon bond cleavage, which is not subject to buffer catalysis, becomes rate-determining. The observed rate then approaches the rate of the carbon-carbon bond cleavage step. The role of the buffer catalyst would presumably be to aid the removal of a proton from an attacking water molecule.

On the basic side of the maximum where the tetrahedral intermediate formation is rate-determining, the tyrphostin hydrolysis is general base catalyzed as described above. At low buffer concentrations where $k_3 \gg \Sigma k_2'[\mathrm{HB}]$ and formation of the tetrahedral intermediate is rate-determining, Eq. 1 reduces to:

$$k = f_{\mathrm{SH}} \Sigma k_1'[\mathrm{B}]$$

$$= f_{\mathrm{SH}}(k_{\mathrm{o}} + k_{\mathrm{OH}}[\mathrm{OH}^-] + k_{\mathrm{CA}}[\mathrm{CA}]) \qquad (8)$$

where k_{o}, k_{OH}, and k_{CA} are the catalytic rate constants for water, hydroxide ion, and chloroacetate ion (CA) attack on the protonated substrate, respectively. From the linear relationship between the observed first-order rate constant and the chloroacetate ion concentration at pH 3.24, a slope of 4.8×10^{-4} s^{-1} M^{-1} was obtained. When the value was divided by the fraction of the substrate in the protonated form at the pH, 1.0×10^{-3} s^{-1} M^{-1} was obtained for the catalytic constant (k_{CA}) for chloroacetate ion. A nearly identical k_{CA} value (9.8×10^{-4} s^{-1} M^{-1}) was obtained when the constant was calculated from the slope of the initial straight line portion of the curve at pH 2.79. Substituting the k_{CA} value in Eq. 8 at the two different pH values of 2.79 and 3.24, the k_{o} and k_{OH} values were calculated to be 4.2×10^{-6} s^{-1} and 1.1×10^{4} s^{-1} M^{-1}, respectively. A logarithmic plot of the catalytic constants (k_{B}) for the catalysis by water, chloroacetate, and hydroxide ions vs the $\mathrm{p}K_{\mathrm{a}}$ for the conjugate acids yielded a slope (β) of approx. 0.6, which is a measure of the sensitivity of the

reaction to the base strength of general base catalysis. The relationship is defined by the Brönsted equation:

$$\log k_B = \log G_B + \beta(pK_a) \quad (9)$$

where G_B is a constant for this particular reaction. It should be noted that the three divergent general bases fit a single plot. The satisfactory fit of the point for water suggests that water reacts as a general base just like the other bases.

At sufficiently high buffer concentrations, an equilibrium exists between the reactant and the tetrahedral addition intermediate so that decomposition of the latter is rate-determining. The

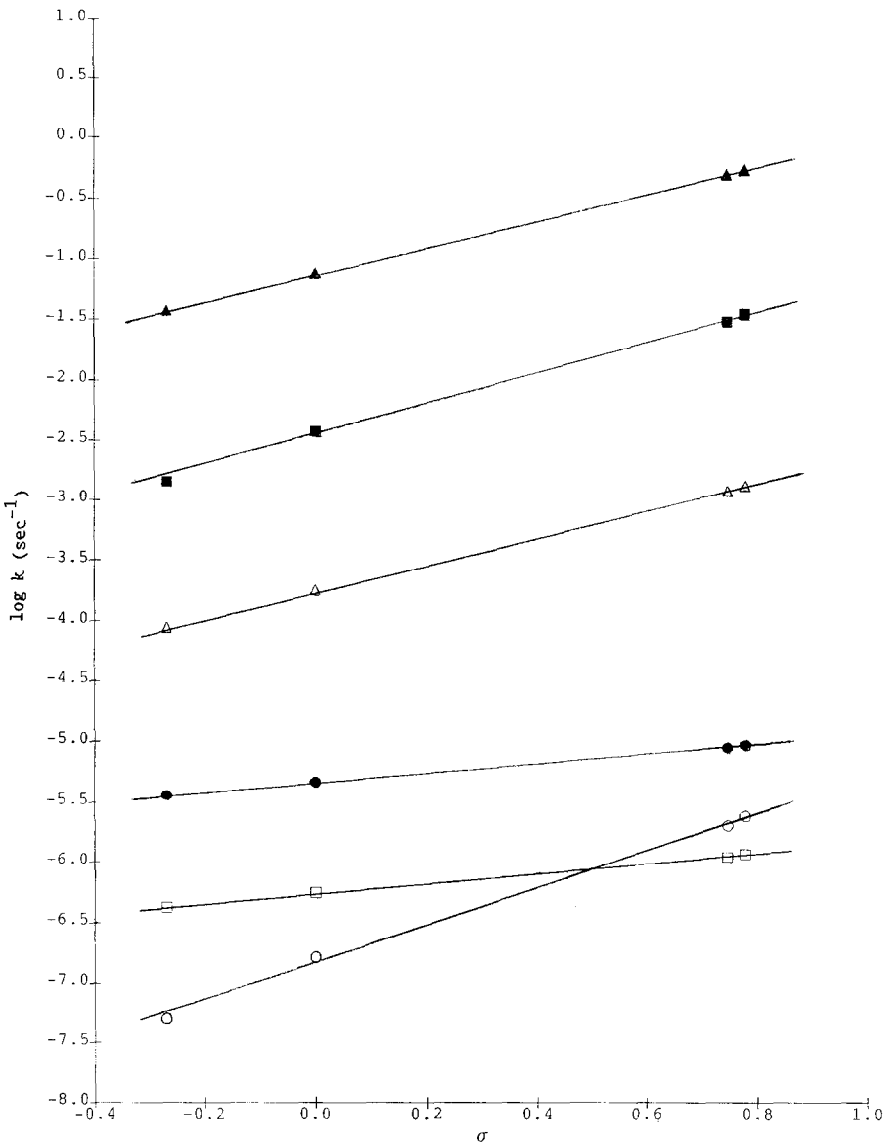

Fig. 4. Dependence of the logarithm of the calculated catalytic and first-order rate constants at three different pH values for the hydrolysis of tyrphostins upon the substituent constants. k_1 (●), k_3/k_H (■), k_4' (▲) and k at pH 1 (○), 4 (□), and 8 (△). The first-order rate constants (k) at the pH values were calculated using Eq. 2 or 6.

equilibrium constant, $K_{SH} = [SHOH][H^+]/[SH^+]$, is related to rate constants (Bell, 1959) as:

$$\frac{k_1}{k_2} = \frac{[SHOH]}{[SH^+]} = \frac{K_{SH}}{[H^+]} \quad (10)$$

At high chloroacetate concentrations, $k_2 = \Sigma k_2'[HB] \gg k_3$ and Eq. 1 reduces to:

$$k = \frac{f_{SH} k_3 K_{SH}}{[H^+]} \quad (11)$$

Eq. 11 is consistent with the pH dependence of the plateau at high buffer concentrations. At constant pH, k approaches a constant value asymptotically as the buffer concentration increases and the rate-determining step changes to breakdown of the tetrahedral intermediate. According to Eq. 11, plateau values of k vs total chloroacetate buffer concentration plots when divided by the fraction of the substrate in protonated form and multiplied by $[H^+]$ should yield a constant value corresponding to $k_3 K_{SH}$.

Substituting $k_2 = k_H[H^+]$ into Eq. 10,

$$K_{SH} = k_1/k_H \quad (12)$$

Consequently, the $k_3 K_{SH}$ value is a product of k_1 and k_3/k_H, and was calculated to be 3.7×10^{-7} s^{-1} M. Since the concentration of chloroacetic acid increases with increasing total chloroacetate buffer concentration, once k_2 in Eq. 1 exceeds k_3, a plateau is observed and Eq. 11 applies.

The rate constant for the hydrolysis of tyrphostins exhibits a dependence upon the nature of the substituents. Tyrphostins possessing electron-withdrawing substituents on the phenyl group bound to the β-carbon atom increase the rate of hydrolysis while those possessing an electron-donating substituent decrease it. It would be expected that electron-withdrawing substituents would increase the carbonium ion character of the β-carbon giving rise to a positive value of Hammett's reaction constant (ρ) in accordance with the proposed mechanism of the nucleophilic attack. The ρ values for k_1, k_3/k_H and k_4' were estimated to be 0.4, 1.2, and 1.4, respectively, from the Hammett plot (Fig. 4).

The dependence of the observed rate constant upon the electronic character of the substituents is seen for three different pH values (Fig. 4). At pH 4, the dependence of the rate on the nature of the substituent ($\rho = 0.4$) results from the reaction of water with the protonated substrate. At pH 1, the observed rate depends on the nature of substituent ($\rho = 1.5$) and the observed ρ value would be largely the result of the substituent effect on the ionization of the intermediate to the dipolar structure (SHOH). Electron-withdrawing substituents would help the oxygen atom of the tetrahedral intermediate lose the proton in acidic solutions. At pH 8, the increase in the rate constant with increasing electron withdrawing nature of the substituents ($\rho = 1.1$) is observed for the hydroxide-ion attack on the β-carbon atom.

4. Acknowledgments

The author wishes to thank Dr V. Windisch for determination of ionization constant, Drs S. Tang and B. Hsu for mass spectral analysis, Ms C. Strohbeck for ^{1}H-NMR, and Ms J. Putnam for elemental analysis. The author also gratefully acknowledges the review of the manuscript by Dr C. Obetz.

5. References

Albert, A. and Serjeant, E.P., *The Determination of Ionization Constants*, Chapman and Hall, London, 1971, pp. 72–75, 103.

Bell, R.P., *The Proton in Chemistry*, Cornell University Press, Ithaca, 1959, pp. 133–135.

Bruice, T.C. and Benkovic, S., *Bioorganic Mechanisms*, Vol. 1, W.A. Benjamin, New York, 1966, p. 9.

Cordes, E.H. and Jencks, W.P., The mechanism of hydrolysis of schiff bases derived from aliphatic amines. *J. Am. Chem. Soc.*, 85 (1963) 2843–2848.

Harned, H.S. and Owen, B.B., *The Physical Chemistry of Electrolyte Solutions*, Reinhold, New York, p. 176.

Jencks, W.P., *Catalysis in Chemistry and Enzymology*, McGraw-Hill, New York, 1969, pp. 477–480.

Jencks, W.P., Mechanism and catalysis of simple carbonyl group reactions. In Streitwieser, A. and Taft, R.W. (Eds), *Progress in Physical Organic Chemistry*, Vol. 2, Interscience, New York, 1964, p. 63.

Koehler, K., Sandstrom, W. and Cordes, E.H., Concerning the mechanism of the hydrolysis and aminolysis of schiff bases. *J. Am. Chem. Soc.*, 86 (1964) 2413–2419.

Lyall, R.M., Zilbertstein, A., Gazit, A., Gilon, C., Levitzki, A. and Schlessinger, J., Tyrphostins inhibit epidermal growth factor (EGF) tyrosine kinase activity on living cells and EGF proliferation. *J. Biol. Chem.*, 264 (1989) 14503–14509.

Martin, R.B., Reactions of carbonyl compounds with amines and derivatives. *J. Phys. Chem.*, 68 (1964) 1369–1377.

Martin, R.B. and Parcell, A., Hydrolysis of 2-methyloxazoline. An intramolecular *O-N*-acyl transfer reaction. *J. Am. Chem. Soc.*, 83 (1961b) 4835–4838.

Martin, R.B. and Parcell, A., Hydrolysis of 2-substituted thiazolines. *J. Am. Chem. Soc.*, 83 (1961a) 4830–4834.

Martin, R.B., Hedrick, R.I. and Parcell, A., Thiazoline and oxazoline hydrolyses and sulfur-nitrogen and oxygen-nitrogen acyl transfer reactions. *J. Org. Chem.*, 29 (1964) 3197–3206.

Patai, S. and Rappoport, Z., Nucleophilic attacks on carbon-carbon double bonds: 1. General considerations: Arylmethylene transfer and cyclodimerization. *J. Chem. Soc.*, (1962) 377–382.